

Autocorrelation Measurements of Green Picosecond Pulses Based on the Two-photon-induced Photocurrent in a Photodiode

Si (Athena) Pan

*Department of Physics, Astronomy and Geophysics,
Connecticut College, New London, CT, 06320*

(Dated: August 8, 2008)

Two commercial photodiodes are tested for two-photon absorption at 520 nm. The results indicate strong linear absorption and negligible two-photon absorption at current power level. Two major types of error associated with autocorrelation measurement based on two-photon induced photocurrent were identified and investigated. Computer simulations show linear absorption can significantly distort the shape of the measured pulse, while misalignment between the reference and delayed beams will yield artificially shortened pulse. Another experiment was conducted to test the misalignment model. The result shows that there are multiple sources for misalignment, which need to be addressed in the future.

I. INTRODUCTION

At Cornell University, the on-going Energy Recovery Linac (ERL) project requires the laser illuminating the photoinjector to produce ultrashort pulses in the range of picoseconds [3]. Furthermore, in order to achieve the goal of producing high charge, low emittance electron beams, the laser pulses must be temporally [3] and spatially [4] shaped. The longitudinal shaping is accomplished through splitting and delaying a pulse in a series of birefringent crystals of different thickness to produce a nearly flat top temporal profile with fast rise and fall times [5]. Such a shaping procedure leads to a series of eight 2-ps pulses with two different polarization directions perpendicular to each other. Due to the polarization sensitivity of second harmonic generation (SHG) process, another approach is needed to characterize shaped pulses. The two-photon-induced photocurrent in a photodiode is a feasible alternative.

The Michelson interferometric second-order autocorrelation has been the conventional method for ultra-short optical pulses measurement. The most frequently used method involves the generation of a phase-matched second-harmonic signal with a frequency doubling crystal [1]. However, it has been demonstrated that second-order autocorrelation measurement can also be attained for femtosecond pulses at 800 nm by using the two-photon-induced free-carrier generation in semiconductors [2].

Commercially available photodiodes often contain impure materials that were introduced during manufacture processes. Such impurity allows linear absorption, which is detrimental for autocorrelation measurement. Part of the research performed this summer is dedicated to testing three commercial UV photodiodes and identifying one, if any, that is suitable for auto-correlation measurement of the ERL laser. The second half of this project is to identify and quantify errors associated with the auto-correlation measurement based on two-photon absorption in a photodiode.

II. ULTRASHORT PULSE AND AUTOCORRELATION MEASUREMENT

Assuming that the shape of the pulse is Gaussian, then the complex wave-function describing these optical pulses is

$$E(t) = Ae^{\frac{-t^2}{2T_0^2}} e^{i\omega t} \quad (1)$$

,where A represents the amplitude of the electric fields, ω is the central angular frequency and T_0 is a constant that determines the width of the pulse [8]. Then the signal from a quadratic detector can be written as

$$A_2(\tau) = \int_{-\infty}^{\infty} I(t)I(t - \tau)dt \quad (2)$$

for the intensity autocorrelation and

$$G_2(\tau) = \int_{-\infty}^{\infty} \{|E(t) + E(t - \tau)|^2\}^2 dt \quad (3)$$

$$= \int_{-\infty}^{\infty} A^4 \left\{ \left| e^{\frac{-t^2}{2T_0^2}} e^{i\omega t} + e^{\frac{-(t-\tau)^2}{2T_0^2}} e^{i\omega(t-\tau)} \right|^2 \right\}^2 dt \quad (4)$$

for a second order interferometric autocorrelation measurement [6]. Plotting the interferometric signal $G(\tau)$ will result in a plot that looks like FIG. 1, which has a peak to background ratio of 8 to 1. The interference fringes measured by the interferometric autocorrelation are too close together to be resolved by any electronic device today, which results in two virtual envelopes (upper and lower) in the plot. The intensity autocorrelation, on the other hand, has a peak to background ratio of 3 to 1.

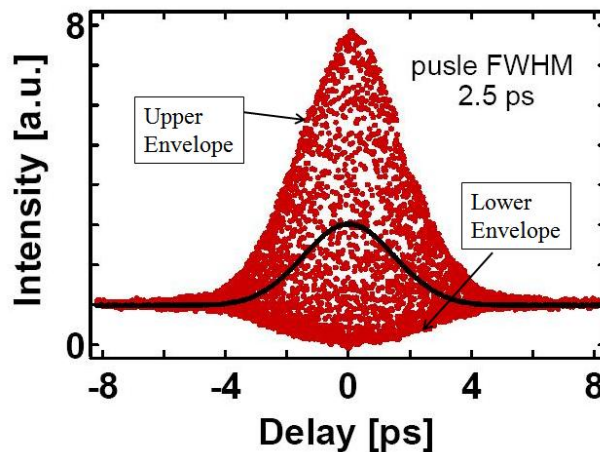


FIG. 1: Autocorrelation trace. Red: interferometric autocorrelation. Black Line: intensity autocorrelation.

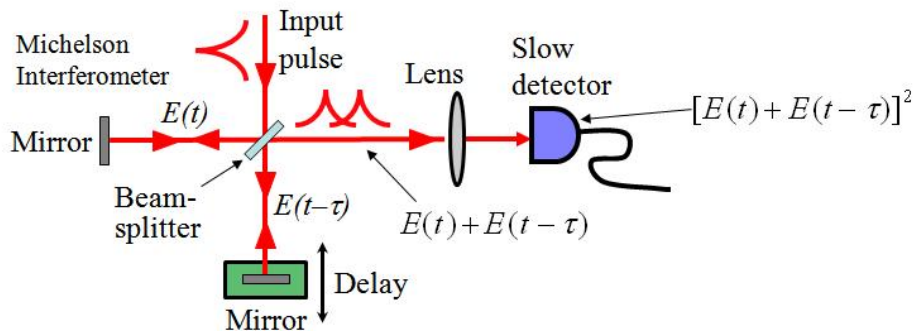


FIG. 2: The typically setup for the autocorrelation measurement with a two-photon absorption photodiode.

III. ERL LASER SYSTEM

The schematic of the ERL laser system is shown in FIG. 3. The system produces a train of 3-ps pulses at 1.3 GHz with an average infrared power of 5 watts. These pulses are then frequency-doubled to output 2-ps pulses at 520 nm with an average power of 250 mW. The energy per pulse is close to 200 pJ.

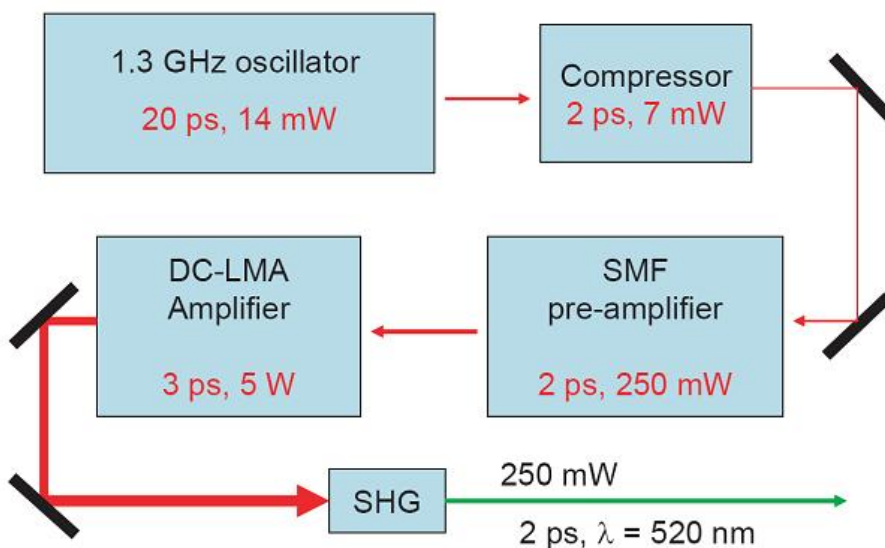


FIG. 3: Schematic of the ERL laser system

IV. TWO-PHOTON ABSORPTION MEASUREMENT IN UV PHOTODIODES

The main objective of this experiment is to measure the photocurrent as a function of the laser beam power. A suitable diode should exhibit a quadratic response signal, which corresponds to the two-photon absorption process. However, due to material impurity within semiconductors, additional electronic states arise between the valence and conduction bands.

Subsequently, it allows linear absorption to happen along with the two-photon absorption. Depending on the amount of impurity within the photodiode, linear absorption can be smaller, equal to or even larger than the two-photon absorption since the probability of absorbing one photon is much higher than that of absorbing two photons continuously.

It is possible to manufacture a photodiode with extremely pure materials. Nonetheless, current commercial photodiodes are not manufactured for application in autocorrelation measurement. Instead, they are designed to emit light when supplied with voltage, in which case impurities do not at all affect the performance of the photodiode. To find a suitable photodiode for laser autocorrelation measurement is not a trivial problem. In fact, the G1116 photodiode that is suitable for $1\ \mu\text{m}$ laser beam measurement [2] was discovered after many unsuccessful trials. It is even more challenging to find a proper photodiode for green laser beams at 520nm, given the fact that fewer photodiodes are manufactured for the UV region due to difficulties in obtaining the proper materials.

The schematic of the experimental setup is shown in FIG 4. The green beam passes through a half-wave plate and a polarizer beam-splitter cube, which when used in combination will allow control on the beam power. The lens reduces the spot size of the beam, which increases the peak intensity of the pulses. Hence, a tighter focusing results in a higher two-photon absorption rate. The pre-amplifier¹ boosts up the current and converts it into voltage.

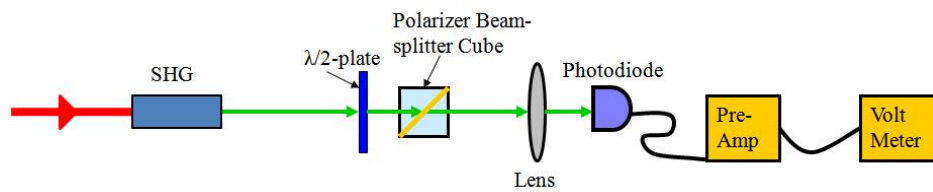


FIG. 4: Schematic of the two-photon absorption experiment setup

The three photodiodes used in this experiment are UVTOP260, UVTOP280 and UVTOP300, which have band gaps of 260nm, 280nm and 300nm, respectively. The UVTOP280, unfortunately, was accidentally damaged while being mounted on the setup. The results of the other two photodiodes are presented in FIG. 5 and 6. Notice the change in peak intensity for difference lens. The 16X lens with a focal length of 11mm is the tightest focusing lens available for this experiment. There is a 40X lens with a focal length of about 2mm. However, the focal length is simply too short for the photodiode to reach the focal point.

The log-log scale fittings of the data show that neither of the photodiodes exhibits quadratic signals at the current power level. Nevertheless, the data points at the high power end show slight deviation from the pure linear signal, which can result from a mixture of linear and quadratic signals. Therefore, it is plausible that these two photodiodes are suitable for higher beam power measurements.

¹ SRS model CR570

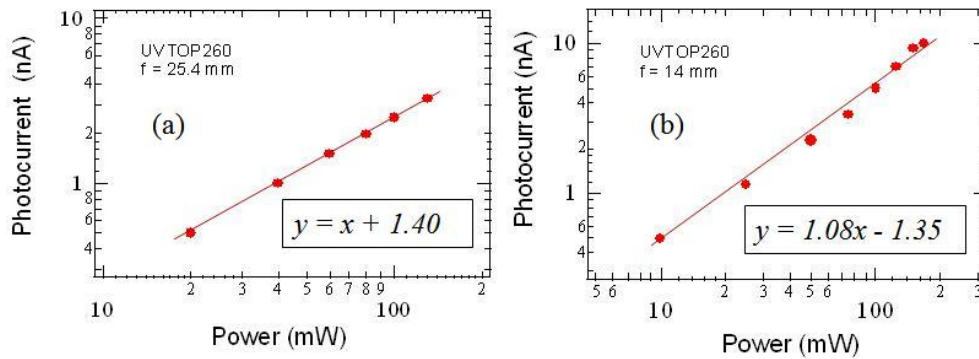


FIG. 5: Measurement with the UVTOP260 diode. (a): spot size $\approx 8\mu\text{m}$, peak intensity $\approx 1.8 \times 10^7 \text{W}/\text{cm}^2$. (b): spot size $\approx 4.6\mu\text{m}$, peak intensity $\approx 6 \times 10^8 \text{W}/\text{cm}^2$. The fittings show that the signals are linear.

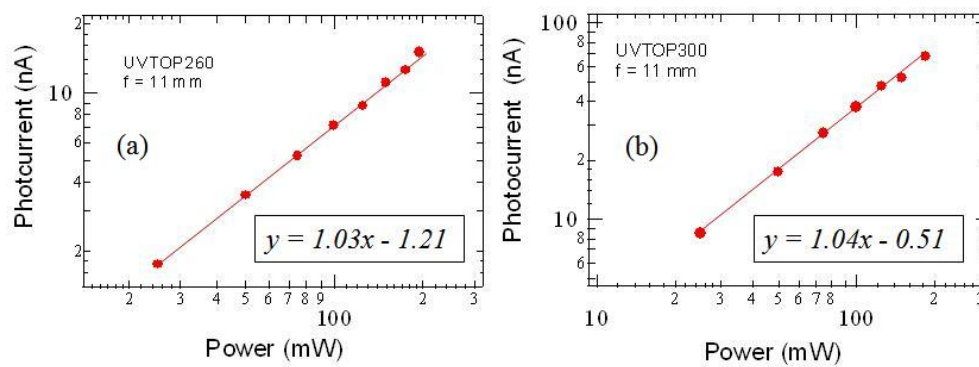


FIG. 6: (a): UVTOP260, 16X lens, spot size $\approx 4\mu\text{m}$, peak intensity $\approx 9.8 \times 10^8 \text{W}/\text{cm}^2$. (b): UVTOP300, 16X lens, spot size $\approx 4\mu\text{m}$, peak intensity $\approx 9.8 \times 10^8 \text{W}/\text{cm}^2$. The fittings show linear signals.

V. ERRORS IN AUTO-CORRELATION MEASUREMENT WITH A TWO-PHOTON ABSORPTION PHOTODIODE

There can be many types of error associated with autocorrelation measurement. Trebino has identified seven of them in his book [7]. Fortunately, since the ERL laser system produces picosecond pulses with narrow spectral bandwidth, most of the errors considered by Trebino are eliminated. Therefore, as far as the measurement of this project is concerned, there are only two major types of error: linear absorption distortion and misalignment while scanning the delay.

A. Linear Absorption Distortion

As mentioned above, linear absorption arises due to material impurity of the photodiode. It has been demonstrated by the experiment in section IV that the linear absorption can sometimes be much stronger than the two-photon absorption. Furthermore, unless the linear absorption is much weaker than the two-photon absorption, the linear signal will

have significant effects on the pulse measurement. In order to demonstrate these effects, a computer simulation is conducted using Mathematica.

Based on the characteristics of the pulses involved in this project, two assumptions are made: first, the shape of the pulse is Gaussian; second, the full width half maximum (FWHM) of the pulse is 2 ps. The linear absorption signal can then be expressed as

$$G_1(\tau) = \int_{-\infty}^{\infty} \{E(t) + E(t - \tau)\}^2 dt \quad (5)$$

An expression for the mixture of the two signals can be found by adding equation 5 to equation 3:

$$G_1(\tau) + G_2(\tau) = \int_{-\infty}^{\infty} \{E(t) + E(t - \tau)\}^2 dt + \int_{-\infty}^{\infty} \{|E(t) + E(t - \tau)|^2\}^2 dt \quad (6)$$

The linear absorption signal is multiplied by a coefficient c , which allows variation in the strength of the linear signal. Let the two signals be equal in strength ($c = 1$), an interferometric autocorrelation measurement is shown in FIG. 7 (a). It is evident that the peak to background ratio is greatly distorted. Instead of 8 to 1, it is now 10 to 2. In addition, the FWHM measured is slightly greater than the correct measurement which comes from a pure second order absorption signal. Similar effects arise in the intensity autocorrelation measurement. (See FIG. 7 (b))

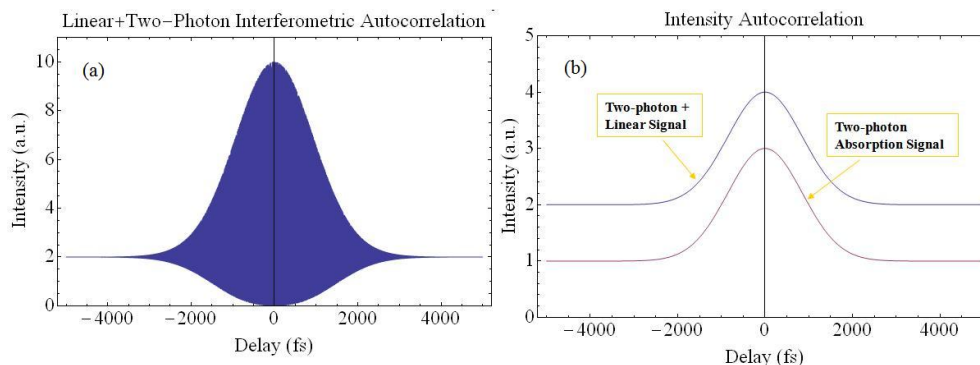


FIG. 7: (a): Linear distortion on interferometric autocorrelation. (b): Linear distortion on intensity autocorrelation.

The relative differences in the peak to background ratio (FIG. 8 (a)), as well as the FWHM (FIG. 8 (b)), are plotted as a function of the coefficient c , which varies from 0.1 to 1. One can immediately appreciate the fact that change in the FWHM is relatively low (5 percent), while variation in the peak to background ratio can be quite large. In theory, it is possible to extract the second order absorption signal from its mixture with the linear signal as long as the ratio of the two signals in strength is known (i.e.: c is known). In practice, however, it is fairly difficult to obtain the ratio between the two signals. Therefore, it is more feasible to test a large number of photodiodes and to obtain one whose two-photon absorption is much higher than its linear absorption.

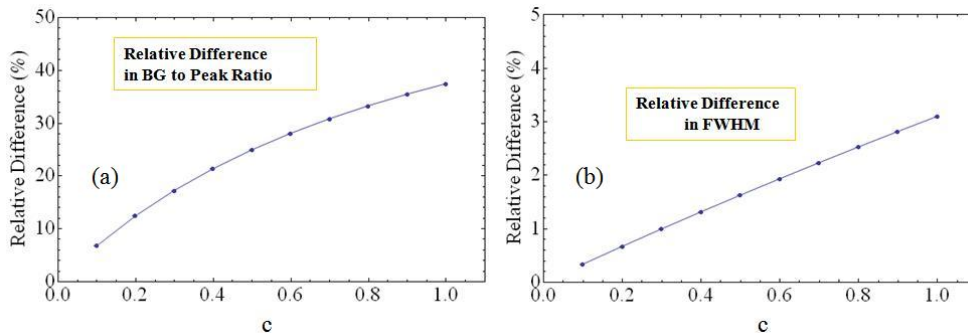


FIG. 8: (a): Relative difference in the peak to background ratio as a function of c , $0.1 \leq c \leq 1$. (b): Relative difference in the FWHM as a function of c , $0.1 \leq c \leq 1$

B. Misalignment When Scanning The Delay

An autocorrelation requires scanning the delay by shaking a mirror. Maintaining a precise overlap between the beams when they recombine is important to the precision of the measurement. However, in practice, it is difficult to accomplish a precise overlap when one of the mirrors is shaking mechanically. The autocorrelator is typically aligned at zero delay, where the reference arm equals to the shaker arm in length. Alignment can be achieved by adjusting all the mirrors for maximum signal energy. However, as illustrated in FIG. 9, if the input beam come in with a slight angle with respect to the y -axis, it will hit the shaking mirror at different spots as the mirror moves back and forth. Hence, the returning beam will hit the beam splitter on different spots as well, which introduces misalignment. Such an effect can happen quite often as the common aligning method is to view the beam directly and do one's best. Additionally, the wobbling effect, which is caused by the random motions of the shaking mirror, can lead to further misalignment [7].

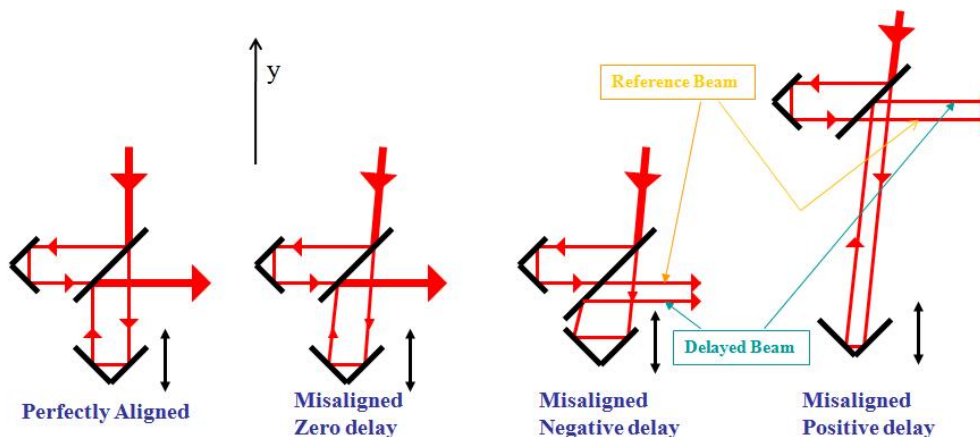


FIG. 9: An illustration of how the misalignment is introduced.

A simple model is built through a computer simulation to investigate this type of error, assuming that both the temporal and spatial shapes of the pulses are Gaussian. It is reasonable to map the spatial misalignment into the time domain. For example, the two delays, -5 ps and 5 ps, can correspond to a maximum negative and positive misalignment, respectively.

Surely, the misalignment will be zero at zero delay where the system is aligned. To be clear, the misalignment is defined as the distance between the centers of the beams. Choosing the x-axis as the misalignment axis, the interferometric autocorrelation can be expressed as

$$G_m(\tau) = \int_{-\infty}^{\infty} \int_{-\infty}^{\infty} \int_{-\infty}^{\infty} A^4 \left\{ \left| e^{-\frac{(x^2+y^2)}{2w_0^2}} e^{-\frac{t^2}{2T_0^2}} e^{i\omega t} + e^{-\frac{((x+\Delta)^2+y^2)}{2w_0^2}} e^{-\frac{(t-\tau)^2}{2T_0^2}} e^{i\omega(t-\tau)} \right|^2 \right\}^2 dt dx dy \quad (7)$$

,where A is again the amplitude, and w_0 determines the spatial width of the pulse.

Assuming the diameter of the beam is $20 \mu\text{m}$, the pulse FWHM is 2 ps and the maximum misalignment is $50 \mu\text{m}$ at -5 and 5 ps delay, the result is shown in FIG. 10 (a). The correct measurement which has no misalignment error is also plotted in the same figure for comparison. This simple computer simulation concludes that artificially shortened pulses will be measured due to misalignment. A similar effect arises in intensity autocorrelation measurement (See FIG. 10 (b)).

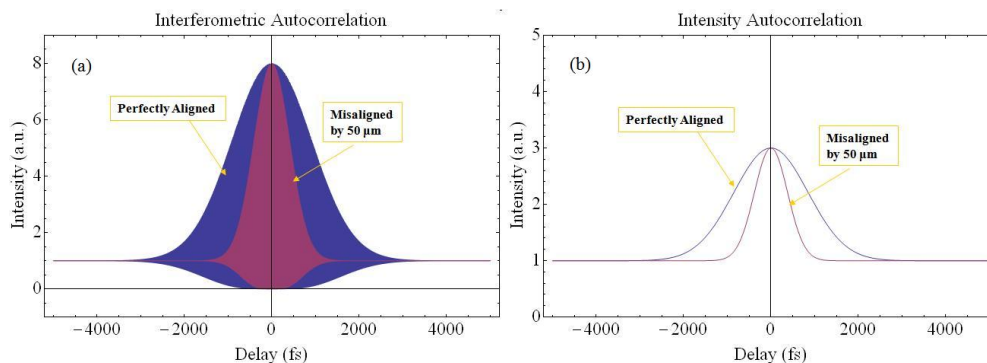


FIG. 10: (a): Comparison between the correct and the misaligned interferometric measurement. The misaligned measurement appears to have shorter duration. (b): Comparison between the correct and the misaligned intensity autocorrelation measurement

Further, the relative difference in FWHM of the pulse between a correct measurement and a misaligned measurement is plotted as a function of the maximum misalignment (See FIG. 11). State-of-the-art instruments today can limit the maximum misalignment effect to within 5 or $10 \mu\text{m}$. Therefore, careful aligning procedures can confine the misalignment error to within 10 percent.

C. Linear Distortion + Misalignment

Combining the two types of error discussed above will yield a pulse that is both distorted and artificially shortened. FIG. 12 are generated for a 2-ps Gaussian pulse with a diameter of $20 \mu\text{m}$. Again, the peak to background ratio of the erroneous measurement is greatly distorted. One can observe the artificially lengthening effect on the pulse envelope by bringing the erroneous plot a unit down (FIG. 12 (b)). In this case, the maximum misalignment is $5 \mu\text{m}$. However, as the maximum misalignment increases, its artificially shortening effect on the pulse envelopes will override the lengthening effect from the linear distortion. Hence, the pulse measured will appear to be shorter than that yielded by a correct measurement.

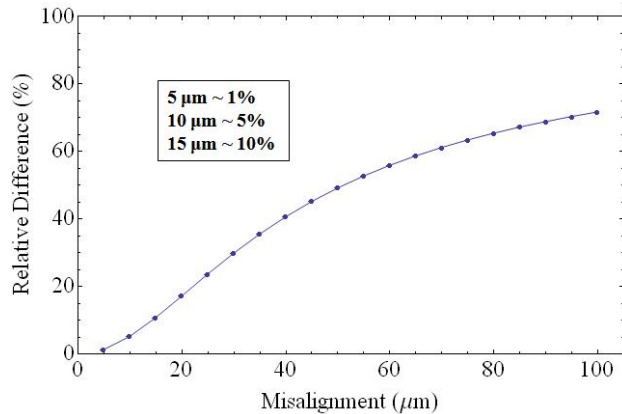


FIG. 11: The relative difference in FWHM between the correct and misaligned measurement is plotted as a function of the maximum misalignment.

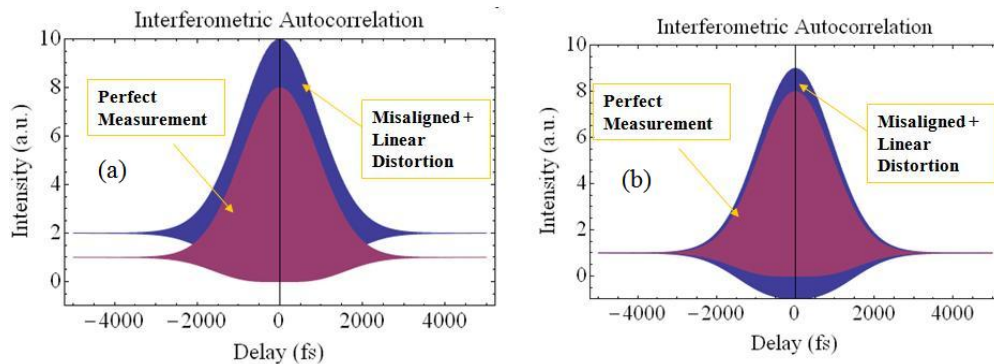


FIG. 12: (a): Simulation plot assuming the beams are misaligned by $5 \mu\text{m}$ and the linear absorption is as strong as the two-photon absorption ($c = 1$). (b): Bringing the misaligned as well as linearly distorted pulse one unit down for comparison.

D. Misalignment Experiment

This experiment is conducted for the purpose of testing the misalignment simulation described in subsection B. The experimental setup is fairly simple. A CCD camera is placed on the output side of the autocorrelator. The resolution of the CCD camera is about $4.5 \mu\text{m}$. The software, which communicates with the CCD, is capable of measuring the stability of the recombined beam after the autocorrelator. Since no suitable photodiode was found for the green laser (section II), this experiment was conducted with an infrared laser operating at 50 MHz [3]. The FWHM of the pulses produced is 3 ps and the average power of the laser is about 60 mW.

After aligning the autocorrelator heedfully, the experiment started with measuring the reference beam only. The result is shown in FIG. 13. Each dot in the figure represents the position of the beam at one instance. The standard deviation from the calculated "center of mass" of the beam can be considered as the misalignment. FIG. 13 shows that the reference beam is relatively stable, with a net σ of about $0.6 \mu\text{m}$.

Then the reference arm is blocked and only the shaker arm is investigated. As shown in FIG. 14 (a), the delayed beam is shifting mostly in the y direction, with a net σ of

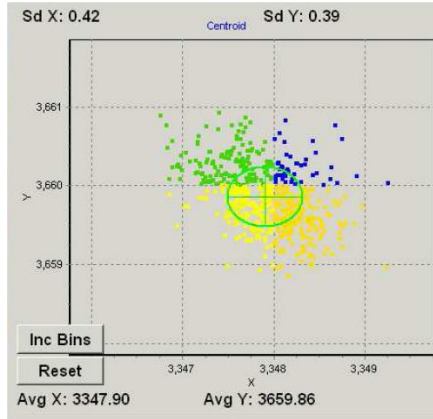


FIG. 13: Measurement of stability of the reference beam from the CCD camera.

about $5 \mu\text{m}$. Then the setup is restored to that for an autocorrelation measurement (see FIG. 2), with the G1116 photodiode as the detector. An intensity autocorrelation trace at this misalignment is measured (See FIG. 14 (b)).

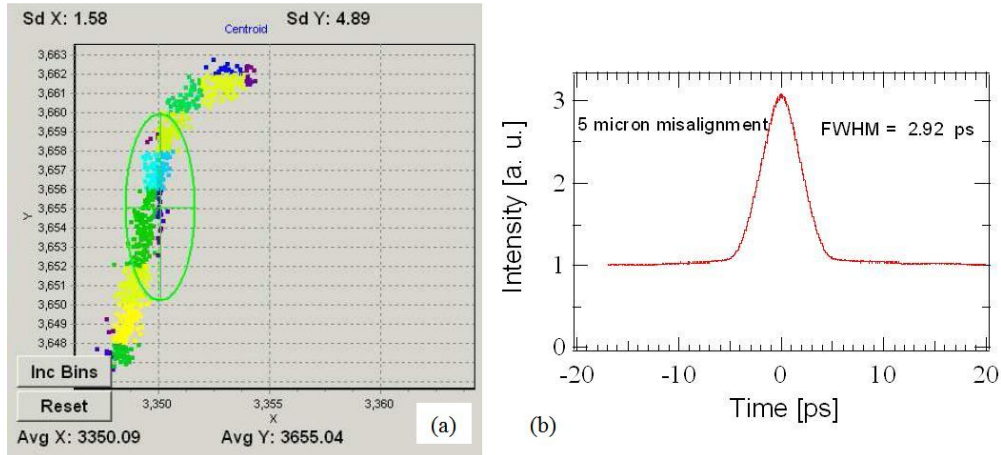


FIG. 14: (a): measurement of the misalignment of the delayed beam from the CCD camera. (b): the trace of the intensity autocorrelation measurement with the G1116 photodiode.

The CCD camera is then restored once again. The shaker mirror is attached to a driving motor through some bearings. By adjusting two screws on the bearings, it is possible to further misalign the beam. FIG. 15 (a) shows the stability of a beam that is further misaligned. The net σ is about $12 \mu\text{m}$. However, it is evident that the beam is not shifting as systematically as in FIG. 14 (a). The sample points shown in FIG. 15 (a) are scattered in all directions. A likely explanation to this is that further misaligning of the beam has disturbed the mechanical stability of the motor-shaker system. Therefore, wobbling effect of the shaking mirror intensifies substantially. An intensity autocorrelation trace is also measured for this misalignment (See FIG. 15 (b)).

The two traces evidently show that the same pulses is measured to be shorter when the beams are further misaligned, which agrees well with the conclusion given by computer simulation. One can further compare the experimental result with the theoretical result by calculating the relative difference in FWHM between the two misalignments, $R_{5,12}$. The

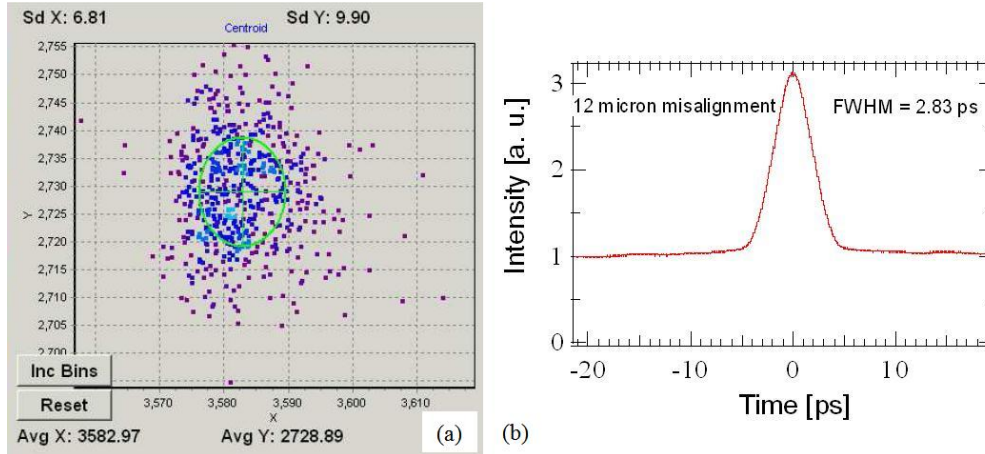


FIG. 15: (a): measurement of the misalignment of the delayed beam from the CCD camera. (b): the trace of the intensity autocorrelation measurement with the G1116 photodiode.

computer simulation in subsection B was repeated for a beam with a diameter of $30 \mu\text{m}$, which turns out to be the spatial size of the beam produced by the laser in this experiment. Knowing the two misalignments, as well as their relative difference in FWHM comparing to the perfectly aligned measurement, one can easily calculate the theoretical $R_{5,12}$ from the computer simulation. The results are shown below:

$$\text{Experimental results : } R_{5,12} = \frac{FWHM_{5\mu\text{m}} - FWHM_{12\mu\text{m}}}{FWHM_{5\mu\text{m}}} \approx 3\text{percent}$$

$$\text{Theoretical results : } R_{5,12} = \frac{FWHM_{5\mu\text{m}} - FWHM_{12\mu\text{m}}}{FWHM_{5\mu\text{m}}} \approx 1.6\text{percent}$$

They differ from each other by a factor of about 2. However, this is reasonable because the computer simulation in subsection B did not account for misalignment due to other effects, such as the shaker mirror wobbling. FIG. 15 (a) shows the existence of these additional effects, which should be addressed in the future so that the theoretical simulation can better match with the experiment.

VI. RESULTS AND DISCUSSION

The two photodiodes tested in this project do not exhibit quadratic response signal at current power level. It remains uncertain whether they will perform better at higher power levels. Continuous search for more suitable photodiodes for green laser autocorrelation measurement is necessary.

Two major types of error associated with two-photon absorption autocorrelation measurement are linear absorption distortion and misalignment while scanning the delay. Linear absorption signal originates from material impurities within the semiconductor. Computer simulation shows that linear absorption can distort the peak to background ratio of the measured pulse. It can also artificially lengthen the pulse duration. Although the artificially

lengthening effect yields small error in the FWHM measured, the peak to background ratio can be significantly distorted depending on the strength of the linear absorption. Therefore, a photodiode must have two-photon absorption signal at least ten times as strong as its linear absorption signal in order to be suitable for any autocorrelation measurement.

The simple misalignment simulation demonstrates that artificially shortened pulses will be measured due to misalignment. This is consistent with the experiment. However, there is a factor of 2 discrepancy between the experimental and theoretical results. This simple simulation did not account for many additional effects that can also lead to misalignment. For example, wobbling effect of the shaking mirror is a very likely candidate. Further investigation is necessary to identify and understand these additional effects. The current computer simulation needs to be modified to account for these effects in order for the theoretical model to better describe reality.

VII. ACKNOWLEDGMENTS

I would like to offer my sincere thanks to my mentor, Dimitre Ouzounov, Ph. D. student, Heng Li, as well as Professor Frank Wise from the Applied Physics and Engineering Department at Cornell University, for their guidance and support through the summer. I would also like to thank NSF for funding this project, and, last but not least, the LEPP REU program for providing me with the opportunity to work and study at Cornell University this summer.

-
- [1] J. C. Diels, J. J. Fontaine, I. C. McMichael, and F. Simoni, *Appl. Opt.* 24,1270-1282 (1985).
 - [2] J. K. Ranka, A. L. Gaeta, A. Baltuska, M. S. Pshenichnikov, and D. A. Wiersma, *Opt. Lett.* 22, 1344-1346 (1997).
 - [3] D. G. Ouzounov, S. Zhou, F. W. Wise, I. V. Bazarov, B. Dunham, and C. Sinclair, *Proceeding of the 2007 Particle Accelerator Conf.*, IEEE, 530-532 (2007).
 - [4] H. Timmers, available from <<http://www.lepp.cornell.edu/ib38/reu/07/timmers.pdf>>.
 - [5] S. Zhou, D. G. Ouzounov, I. Bazarov, B. Dunham, C. Sinclair, and F. W. Wise, *Appl. Opt.* 46, 1-5 (2007).
 - [6] J. C. Diels, W. Rudolph, *Ultrashort Laser Pulse Phenomena*, (Academic, CA, 1996), Chap. 1.
 - [7] R. Trebino, *Frequency-Resolved Optical Gating: The Measurement of Ultrashort Laser Pulses*, (Kluwer Academic, MA, 2000), p. 92-96.
 - [8] B.E.A. Saleh, M. C. Teich, *Fundamentals of Photonics*, (John Wiley and Sons, NJ, 2007), p. 937-940.